New insights from Raman MicroSpectroscopy and Scanning Electron Microscopy on the microstructure and chemical composition of vestibular and lingual surfaces in permanent and deciduous human teeth

# New insights from Raman MicroSpectroscopy and Scanning Electron Microscopy on the microstructure and chemical composition of vestibular and lingual surfaces in permanent and deciduous human teeth

Giulia Orilisi[a], Riccardo Monterubbianesi[a], Valentina Notarstefano[b], Vincenzo Tosco[a], Flavia Vitiello[a], Giampaolo Giuliani[c], Angelo Putignano[a], Giovanna Orsini[a*]

[a] Department of Clinical Sciences and Stomatology, Polytechnic University of Marche, Ancona, Italy; g.orilisi@pm.univpm.it (Giu.O.); r.monterubbianesi@pm.univpm.it (R.M.); v.tosco@pm.univpm.it (V.T.); flavit94@gmail.com (F.V.); a.putignano@staff.univpm.it (A.P.)

[b] Department of Life and Environmental Sciences, Polytechnic University of Marche, Ancona, Italy; v.notarstefano@staff.univpm.it (V.N.)

[c] Department of Materials, Environmental Sciences and Urban Planning, Polytechnic University of Marche, Ancona, Italy; g.p.giuliani@univpm.it (G.G.)

*Corresponding Author:
Prof. Giovanna Orsini, Polytechnic University of Marche, Department of Clinical Sciences and Stomatology (DISCO), Via Tronto 10, 60126, Ancona, Italy. Phone number: +39 3472483290; E-mail address: g.orsini@univpm.it; giovorsini@yahoo.com

**Abstract**

Teeth are characterized by a specific chemical composition and microstructure, which are also related to their nature, permanent and deciduous, and to the sides, lingual and vestibular. Deeper knowledge in this topic could be useful in clinical practice to develop new strategies in restorative dentistry and in the choice of materials with the best performances. In this study, Raman MicroSpectroscopy (RMS), Scanning Electron Microscopy (SEM), Energy Dispersive X-ray Spectrometry (EDS), and Vickers MicroHardness (VMH) were exploited to: (1) characterize the microstructure and the chemical/elemental composition of permanent and deciduous human teeth, also in terms of lingual and vestibular sides, and (2) validate a new multidisciplinary analytical approach, for obtaining multiple information on calcified tissues. All applied techniques evidenced differences between permanent and deciduous teeth both in the lingual and vestibular sides. In particular, scanning electron micrographs identified areas with an irregular appearance in the vestibular and lingual sides, which presented also different VMH values. Moreover, RMS and EDS displayed a different chemical/elemental composition in outer and inner enamel and dentin, in terms of Mineral/Matrix, Crystallinity, Carbonates/phosphates, and concentrations by weight (%) of calcium, phosphorous, carbon, magnesium, and sodium. A good linear correlation was found between RMS spectral profiles and EDS and VMH measurements, suggesting that RMS may be considered a useful and non-destructive diagnostic tool for obtaining multiple information on calcified tissues.

**Keywords:** enamel, dentin, deciduous teeth, permanent teeth, Raman microspectroscopy, analytical techniques

## 1. Introduction

Enamel and dentin are the major components of the human dental crown, produced by ameloblasts and odontoblasts, respectively, and exhibiting different function, composition, and structure [1]. Enamel plays an essential role in protecting teeth against mechanical and chemical actions [2]. It is the hardest and most highly mineralized tissue in the human body, with a composition up to 96-97% by weight of inorganic matter, 2-3% of water, and only 1% of non-collagenous organic material [2,3]. Its microstructure mainly consists of carbonated and fluorinated hydroxyapatite (HA) crystals, arranged in prisms, which run approximately perpendicular from the dentin-enamel junction towards the tooth surface [4].

Dentin is located under the enamel layer, and is less mineralized than enamel [5]; it supports enamel, preventing it from fracturing during occlusal loading and protecting the pulp chamber from external dangerous stimuli [5]. Dentin mineral content is approximately 70% by weight, whereas the organic matrix, mainly composed of cross-linked type I collagen and Amide I, is around 20% [6]. As a result, dentin is a typical composite material formed by inorganic HA crystals and organic collagen matrix proteins [7].

The primary dentition is substituted by the permanent one during adolescence [8]. The deciduous crown average growth is from 6 to 14 months, whereas the permanent one is from 3 to 4 years. Differences in terms of chemical and microstructural features between permanent and deciduous teeth (Pe and De, respectively) play an important role in specific conditions, such as caries, susceptibility to demineralization, abrasion and erosion processes, and etching procedures [9,10]. Although the first study, reporting micrographs of dental enamel, goes back in the scientific literature to more than a century, its composition and organization are still debated [11]. It has been documented that Pe and De display a different enamel microstructure; in fact, Pe are composed of thicker and richer prisms, while De are characterized by enamel with a lower density of prismatic crystal structures, smaller prisms, fewer mineral substances and major organic content [12,13]. As regards dentin, both Pe and De present a similar arrangement of the organic content; conversely, some differences were highlighted in the mineral one [6,8], probably causing the faster caries progression, observed more in primary than in permanent dentition [14]. Additionally, the pulp chamber of De appeared bigger than its successor teeth and the dentin secretion and pulpar repair activity decreased with aging [8].

Raman MicroSpectroscopy (RMS) is a non-destructive and label-free vibrational technique that has been employed, in the last years, by an increasing number of researchers, to study mineralized tissues, such as bones and teeth, since it is sensitive both to the mineral and to the organic components

[11,15,16]. In dentistry, it is mainly used in the restorative field to study teeth structure, dentin-adhesive-composite interface as well as caries progression [6,15]. Scanning Electron Microscopy (SEM) is a microscopy-based technique, which lets obtain qualitative information on the morphology of the samples due to its ability to create high-resolution images of hard surfaces [17,18]. SEM represents an important tool for research in dentistry, since it is well suited for the study of the microstructure of tooth tissue, such as enamel and dentin [19]. Moreover, Energy Dispersive X-ray Spectrometry (EDS) is used to determine the mineral content of dental hard tissues [20,21]. The main advantage of this system is its capability to provide an accurate elemental analysis, adding more information to the RMS data [22]. Finally, Vickers MicroHardness (VMH) test provides information regarding the mechanical behavior of dental enamel [16]. The knowledge of the mechanical characteristics of dental enamel, associated to its chemistry and microstructure, could provide valuable insights regarding the development of new oral treatments and dental reconstructions [23].

To date, few studies and with contradictory results are reported in literature on the structural differences between vestibular and lingual surfaces of Pe and De [4,13]. Given the lack of homogeneous results in calcified tissues field, in this study, a multidisciplinary approach, including RMS, SEM, EDS, and VMH were exploited to characterize the microstructure and chemical/elemental composition of enamel and dentin in Pe and De, by considering both lingual and vestibular sides.

## 2. Materials and Methods

### *2.1 Samples collection and preparation*

The study was performed on eight deciduous and eight permanent human teeth collected at the Section of Stomatology of the Polytechnic University of Marche, Ancona, Italy. Teeth were surgically extracted for therapeutic purposes. Deciduous teeth (De) came from 10-11 years old subjects, whereas the permanent ones (Pe) were extracted from 50-55 years old subjects. According to the Local Ethical Committee guidelines and the WMA - Declaration of Helsinki (2018) [24], an informed consent was signed from all patients that aware that their hard dental tissues, as discard of the surgical procedures, would be used for research purposes. After surgical extraction, teeth were washed in an ultrasonic bath with distilled water for 2 minutes, in order to remove the blood and biological remains, and then carefully examined to exclude the presence of lesions and decays, including hypoplastic defects and cracks. Since three De and Pe exhibited one of these features, they were excluded from the study. Thus, the selected De (N=5) and Pe (N=5) were stored in artificial saliva (Biotène Oral Balance, Biopharm Sas, Peschiera Borromeo, Italy), which was daily changed.

Lingual and vestibular sides of Pe (PeL-S and PeV-S, respectively) and De (DeL-S and DeV-S, respectively) were submitted to VMH, RMS, and SEM measurements. Then, teeth were cut in the vestibular-lingual direction, starting at the level of the occlusal fissure, to get two halves for each

tooth; a diamond saw (Buehler Isomet 1000, USA) with copious water irrigation was used. The cut surfaces were flattened and polished first with OptiDisc (Kerr, Bioggio, Switzerland), using the sequence Extra-Coarse, Coarse/Medium, Fine and Extra-Fine, and then furtherly polished with a diamond powder dispersion (particle size ranging from 6 to 1 µm) [21,25]. Specific areas corresponding to the outer enamel (OE), inner enamel (IE), and dentin (D), taken at a distance of 700 µm from the dentin-enamel junction, of vestibular and lingual sides were identified and analyzed. More in detail, the following areas were studied: permanent lingual outer enamel (PeL-OE); permanent lingual inner enamel (PeL-IE); permanent lingual dentin (PeL-D); permanent vestibular outer enamel (PeV-OE); permanent vestibular inner enamel (PeV-IE); permanent vestibular dentin (PeV-D); deciduous lingual outer enamel (DeL-OE); deciduous lingual inner enamel (DeL-IE) deciduous lingual dentin (DeL-D); deciduous vestibular outer enamel (DeV-OE); deciduous vestibular inner enamel (DeV-IE), and deciduous vestibular dentin (DeV-D).

The detailed methodological processing of the present study and the samples' legend are simplified in Fig. 1.

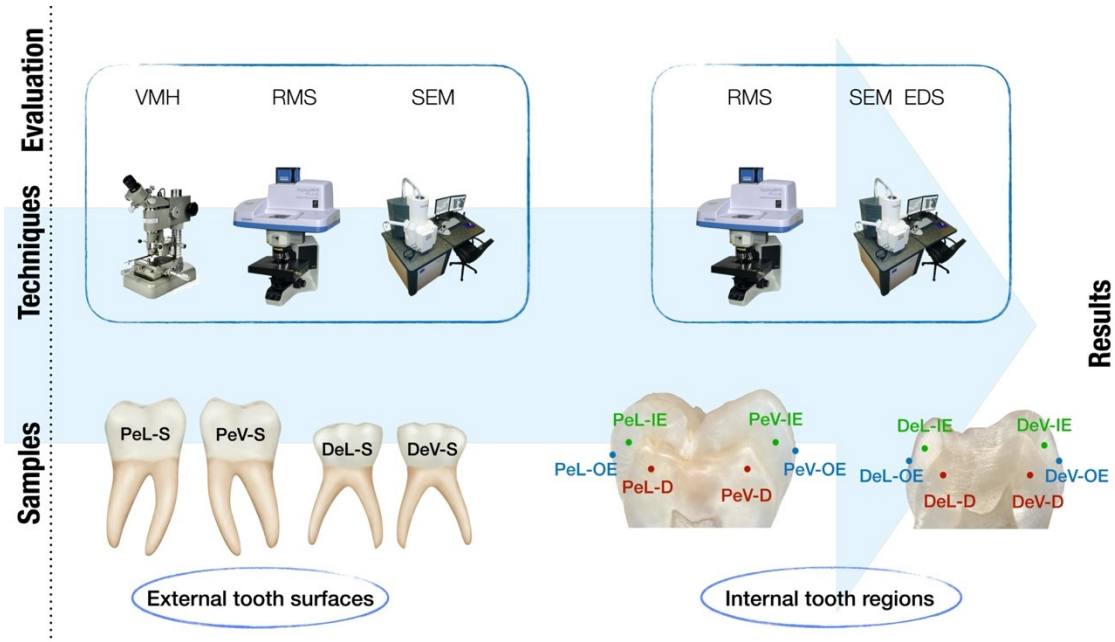


**Fig. 1**. The methodological processing followed in the study. Analytical techniques used on the external surfaces and internal regions of teeth: Vickers MicroHardness test (VMH), Raman MicroSpectroscopy (RMS), Scanning Electron Microscopy (SEM) and Energy Dispersive X-ray Spectrometry (EDS).

*2.2 Microhardness measurements*

VMH test was performed using a Remet microhardness tester HX-1000 (Remet S.A.S., Casalecchio di Reno, Italy). In the center of the crown of each intact Pe and De, specific enamel areas

corresponding to PeL-S, PeV-S, DeL-S and DeV-S were selected (Fig. 1). On each area, three indentations were performed using a pyramid-shaped diamond loaded with 50 g for 15 sec; the distance between one indentation and another was approximately 100 μm [8]. After removing the load, the values of the indentation diagonals were evaluated by using a microscope; the area of the sloping surface was obtained and used to determine the corresponding hardness value. For each experimental group, 15 values were collected from the vestibular surfaces and 15 from the lingual ones.

*2.3 RMS measurements and data analysis*

A Horiba Jobin-Yvon XploRA Nano Raman Microspectrometer, equipped with a 785-nm diode laser was used as a source. All RMS measurements were acquired by using a 5× objective (Olympus, Tokyo, Japan). The spectrometer was calibrated to the 520.7 $cm^{-1}$ line of silicon prior to spectral acquisition. A 600 lines per mm grating was chosen. A 200 μm confocal pinhole was used for all measurements. The spectra were dispersed onto a 16-bit dynamic range Peltier cooled CCD detector. RMS measurements were performed on the lingual and vestibular superficial enamel of intact teeth and on their internal regions, focusing on outer and inner enamel and dentin.

*2.3.1. Tooth external surfaces*

Three RMS point/spectra were acquired on each intact tooth, close to the areas used for VMH measurements (PeL-S, PeV-S, DeL-S, and DeV-S) (Fig. 1). The spectral range from 650 to 1800 $cm^{-1}$ was chosen and spectra were acquired for 3×10 seconds at each point. Raman spectra displayed homogeneous profiles. Raman spectra were smoothed using 5 smoothing points, baseline-corrected with the polynomial method (2 iterations) (OPUS 7.5 software, Bruker Optics GmbH, Ettlingen, Germany), and then submitted to multivariate analysis. More in detail, Principal Component Regression (PCR) was exploited to relate the modification in the Raman spectral profiles of superficial enamel of PeL-S, PeV-S, DeL-S, and DeV-S intact teeth to microhardness values, by following a two-step procedure: first, the exploratory analysis of Principal Component Analysis let identify PC scores, and then these scores were used to build a regression model to link the spectral information with VMH (OriginPro 2018b, OriginLab Corporation) [26].

*2.3.2. Tooth internal regions*

Raman mapping was performed on PeL-OE, PeL-IE, PeL-D, PeV-OE, PeV-IE, PeV-D and DeL-OE, DeL-IE, DeL-D, DeV-OE, DeV-IE, DeV-D (Fig. 1). Raman maps were acquired with the same parameters described in the previous section, on rectangular areas (241.5 μm × 167 μm), with a step size of ~15 μm, for a total number of 192 spectra. On each Raman map, the following values were calculated: the area of the band centered at 1660 $cm^{-1}$ (spectral range 1655-1707 $cm^{-1}$), representing the Amide I band of proteins ($A_{1660}$) [27,28]; the area, intensity, and full width at half maximum of

the band centered at 960 $cm^{-1}$ (spectral range 929-976 $cm^{-1}$), assigned to the stretching of $PO_4^{3-}$ groups of HA ($A_{960}$, $FWHM_{960}$, and $I_{960}$) [6,16]; the intensity of the band centered at 1070 $cm^{-1}$ (spectral range 1051-1088 $cm^{-1}$), assigned to the stretching of $CO_3^{2-}$ groups ($I_{1070}$) [6,11,29] (Labspec 6 software, Horiba Scientific). These values were employed to generate false-color images showing the spatial distribution of the following spectral features: Mineral/Matrix ($A_{960}/A_{1660}$), Crystallinity (inversely proportional to $FWHM_{960}$), and C/P (carbonates/phosphates, $I_{1070}/I_{960}$) [6].

Finally, from each Raman map, spectra were extracted and submitted to preprocessing procedures, including baseline correction (2 iterations, polynomial method), smoothing (5 points), and vector normalization (OPUS 7.5 software). Preprocessed spectra were submitted to Principal Component Regression (PCR), to relate the changes in Mineral/Matrix, Crystallinity, and C/P, to the concentrations by weight (%) of Ca (calcium), P (phosphorous), O (oxygen), C (carbon), Mg (magnesium) and Na (sodium), obtained by EDS (see paragraph 2.4) (OriginPro 2018b, OriginLab Corporation).

*2.4 SEM and EDS measurements*

SEM and EDS measurements were performed using a Zeiss Supra 40 field-emission electron microscope. Measurements were performed on the same samples previously analysed by VMH and RMS (Fig. 1). Samples were assembled in a sample holder and metalized with vacuum precipitation of a gold film on the dental surface [20]. The obtained micrographs were evaluated descriptively, observing the variations in the micromorphology of enamel and dentin in the analyzed samples.

*2.4.1 Tooth external surfaces*

SEM micrographs of the vestibular and lingual external enamel of intact Pe and De were obtained at magnifications of 30000× (3 zones for each tooth). SEM operated at 20 kV and at 8.5 mm working distance.

*2.4.2 Tooth internal regions*

Three scanning electron micrographs were obtained at magnifications of 2000× and 8000× for each area, as described above. SEM operated at 30 kV and at a 12 mm working distance. To calculate the number of dentinal tubules per $mm^2$, all the tubules contained in one photograph were counted. Where tubules intersected the edges of the photograph, only those that intersected the top and right-hand margins were included in the total. On each area evaluated by SEM, the EDS analysis was carried out, using the following operating parameters: 15 mm working distance, 25 kV accelerating voltage, and 400× magnification. On each zone, three spot measurements were performed. The concentrations by weight (%) of Ca (Calcium), P (Phosphorous), O (Oxygen), C (Carbon), Mg (Magnesium), and Na (Sodium) were evaluated.

*2.5. Statistical analysis*

Normally distributed data deriving from Raman spectra, VMH, and EDS analysis were presented as mean ± standard deviation (SD). Significant differences between tooth regions and experimental groups were determined by means of factorial analysis of variance (one-way ANOVA), followed by Tukey's multiple comparisons test, using the statistical software package Prism6 (Graphpad Software, Inc. USA). One-way ANOVA compares the means of all experimental groups, in order to make inferences about the population means. Statistical significance was set at $p < 0.05$. Data obtained from VMH and EDS measurements were submitted to multivariate analysis and correlated, as reported below, with results derived from RMS measurements (OriginPro 2018b, OriginLab Corporation).

## 3. Results

*3.1 Analysis of the external tooth surface*

By considering VMH in all the analysed groups, the lowest value was found in DeL-S ($p<0.05$), while the highest ones were displayed by the vestibular sides of both Pe and De (PeV-S and DeV-S, $p<0.05$) (Fig. 2A). Moreover, a statistically significant difference was observed between lingual and vestibular sides of both Pe and De (PeL-S and PeV-S, $p<0.05$; DeL-S and DeV-S, $p<0.05$). However, PeV-S and DeV-S showed no significant differences ($p>0.05$).

By the analysis of Raman spectra reported in Fig. 2B, the following peaks were highlighted: 1660 $cm^{-1}$ (Amide I peak of proteins), 1070 $cm^{-1}$ ($CO_3^{2-}$ groups), and 960 $cm^{-1}$ ($PO_4^{3-}$ groups of HA) [6]. Moreover, Fig. 2C and Fig. 2D respectively display the obtained PC scores plot and the PC1 and PC2 loadings. Complete segregation of spectra from Pe and De was obtained along PC1 (75.2% of explained variance); the lingual and the vestibular sides of Pe were perfectly discriminated by PC2 (12.1% of explained variance); DeV-S and DeL-S appear as two close clusters, although not completely divided by PC2. The loading spectra of PC1 and PC2 axes report how the most discriminant spectral features are ascribable to the above described Raman peaks, together with the peak centred at 1005 $cm^{-1}$ (assigned to the vibration of phenylalanine of organic matrix). Then, PC scores were used to create a regression model able to correlate the spectral information with VMH; a good linear correlation was found ($R^2= 0.953$).

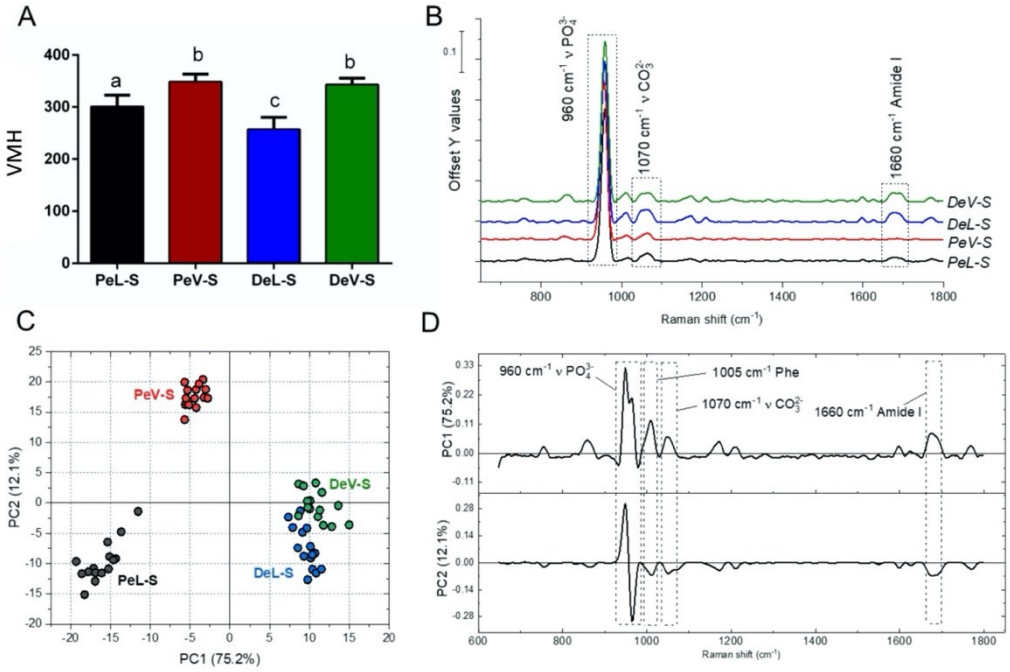


**Fig. 2.** Analysis of the external enamel surfaces of lingual and vestibular sides of Pe and De. (A) Vickers MicroHardness analysis (VMH) (one-way ANOVA and Tukey's multiple comparisons test; different uppercase letters represent the statistically significant difference, $p < 0.05$). (B) Average Raman spectra (dotted rectangles highlight the three peaks of interest; for better viewing, spectra are offset along the y-axis). (C) PCA scores plot calculated for PeL-S, PeV-S, DeL-S, and DeV-S spectra, and (D) corresponding PC1 and PC2 loading spectra.

SEM analysis was exploited to descriptively evaluate and compare the micromorphology of vestibular and lingual external surfaces of Pe and De (Fig. 3). At a magnification of 30000×, PeV-S showed a more regular pattern, with enamel-like crystal structure and perikymata, with respect to PeL-S, in which some irregularities were detected. Furthermore, PeV-S seemed to be smoother than DeV-S, which displayed a partial loss of the enamel surface integrity. DeL-S appeared the most irregular with loosely packed crystals and dark areas.

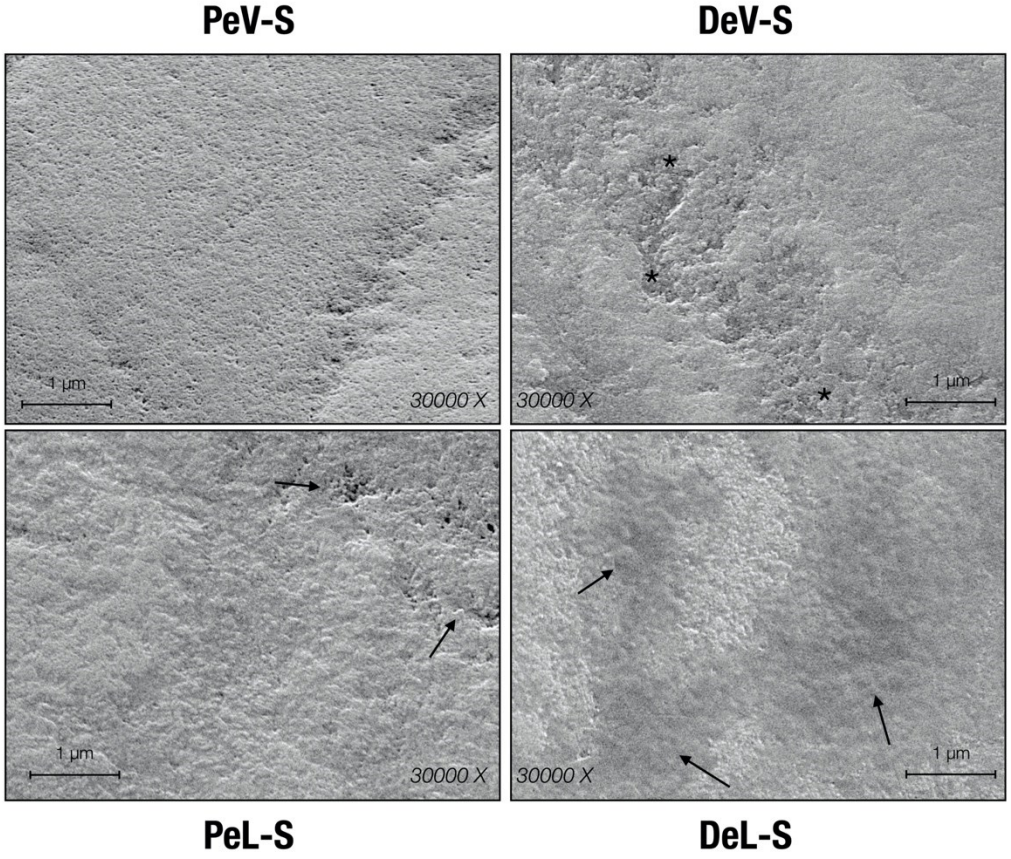


**Fig. 3.** Scanning electron micrographs of the external enamel surfaces of vestibular and lingual sides of representative Pe and De. Micrographs were collected at 3000× original magnification. PeV-S showed the smoothest surface with an enamel-like crystal structure and perikymata. DeV-S displayed a minimal loss of enamel surface integrity (black asterisks). In PeL-S a non-homogeneous area was highlighted with the presence of a partial core prisms dissolution (black arrow). DeL-S showed some areas with partial loss of perikymata (black arrow), more evident with respect to PeV-S and DeV-S.

*3.2 Analysis of tooth internal regions*

Raman results were summarized in Fig. 4. False-color images, representing the spatial distribution of Mineral/Matrix ($A_{960}/A_{1660}$), Crystallinity (inversely proportional to $FWHM_{960}$), and C/P (carbonates/phosphates, $I_{1070}/I_{960}$) spectral features, were created; different color scales were adopted, according to minima and maxima values of the analyzed ratios within each map (Fig. 4A-H). As regards Pe, higher Mineral/Matrix values were highlighted in PeL-IE and PeV-IE than to outer ones (PeL-OE and PeV-OE), while, in both lingual and vestibular surfaces, lower values were characteristic of dentin (PeL-D and PeV-D) with respect to inner enamel (PeL-IE and PeV-IE) (Fig. 4B). Regarding Crystallinity in both lingual and vestibular surfaces, homogeneous values were distributed in PeL-OE, PeV-OE, PeL-IE and PeV-IE, while lower values were observed in PeL-D and PeV-D with respect to PeL-IE and PeV-IE (Fig. 4C). Lower C/P values were showed in PeL-IE and PeV-IE with respect to outer enamel (PeL-OE and PeV-OE) and dentin (PeL-D and PeV-D)

(Fig. 4D). As regards De, almost homogeneous Mineral/Matrix values were distributed in lingual outer (DeL-OE) and inner (DeL-IE) enamel, while in the vestibular surface, high values were observed in DeV-IE respect to DeV-OE; lower values were evidenced in both lingual and vestibular dentin (DeL-D and DeV-D) respect to DeL-IE and DeV-IE (Fig. 4F). Regarding Crystallinity, in both lingual and vestibular surfaces, almost homogeneous values were displayed in DeL-OE, DeV-OE, DeL-IE and DeV-IE, while lower values were observed in dentin (DeL-D and DeV-D) with respect to inner enamel (DeL-IE and DeV-IE) (Fig. 4G). In both lingual and vestibular surfaces, low C/P values were mainly distributed in the inner enamel (DeL-IE and DeV-IE) with respect to outer enamel (DeL-OE and DeV-OE) and dentin (PeL-D and PeV-D) (Fig. 4H).

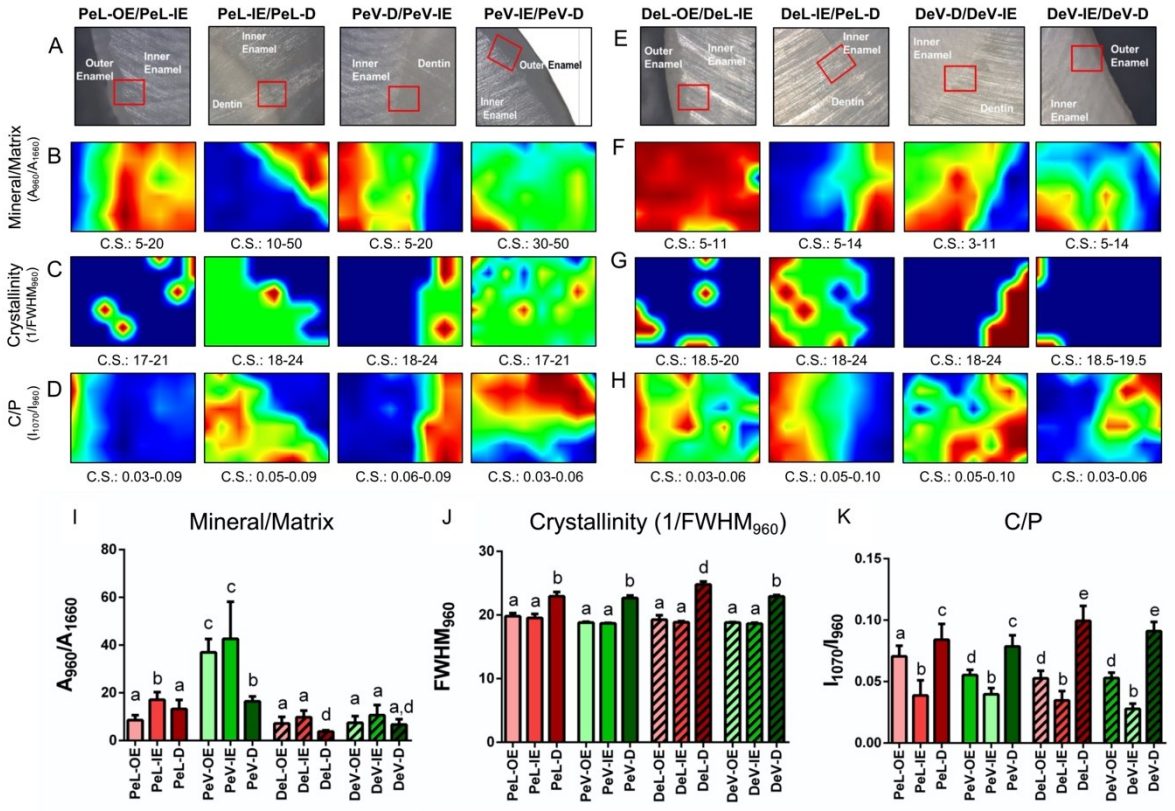


**Fig. 4**. Raman mapping analysis of representative areas at the outer/inner enamel and inner enamel/dentin interfaces in vestibular and lingual surfaces of Pe and De. (A,E) Photomicrographs reporting the selected areas (red rectangles, 241.5 µm × 167 µm) and corresponding false-color images (241.5 µm × 167 µm) showing the topographical distribution of (B,F) Mineral/Matrix ($A_{960}/A_{1660}$), (C,G) Crystallinity (inversely proportional to $FWHM_{960}$), and (D,H) C/P (carbonates/phosphates, $I_{1070}/I_{960}$) spectral features. Different color scales (C.S.) were used for a better interpretation of the data: exact values are reported below each map (black/blue color corresponds to the lowest values, green intermediate and red/dark red to the highest ones). Statistical analysis of the numerical variation of (I) Mineral/Matrix, (J) Crystallinity, and (K) C/P calculated values. Data are presented as mean ± SD. Different letters above box charts indicate statistically significant differences among groups ($p < 0.05$; one-way ANOVA and Tukey's multiple comparison test).

Regarding Mineral/Matrix ($A_{960}/A_{1660}$) (Fig. 4I), Pe showed significantly different values between lingual and vestibular surfaces, with the highest values found in the inner and outer enamel of the vestibular surface; De displayed comparable values in the vestibular and lingual surfaces, except for the dentin region of the lingual surface, which displayed a significantly lower value. As regards Crystallinity (inversely proportional to $FWHM_{960}$) (Fig. 4J), statistically comparable values were displayed by inner and outer enamel of all the analyzed samples; respect to enamel, dentin showed significantly lower values, in particular in deciduous lingual samples. Carbonates/phosphates (C/P, $I_{1070}/I_{960}$) values (Fig. 4K) displayed the lowest values in the inner enamel of all the analyzed surfaces, significantly higher values in outer enamel, and the highest values in dentin; interestingly, the highest one was showed by dentin of deciduous lingual surface.

SEM analyses were summarized in Fig. 5. At 2000× magnification, PeV-IE showed a more regular surface compared to PeL-IE and DeV-IE, in which a partial loss of enamel-like crystal structure and perikymata was observed, especially in micrographs at high magnification (8000×). The tubule density in dentin appeared higher in PeV-D with respect to the PeL-D one (19600 tubules/$mm^2$, 7400 tubules/$mm^2$, respectively). Thus, the lingual surface contained more intertubular dentin matrix. Moreover, the tubules orientation was different: in the lingual side, tubules appeared more diagonally with respect to the pulp chamber, compared to the vestibular one, in which they seem to be more parallel (Fig. 5A). DeV-IE and DeL-IE appeared irregular, with a wavy architecture, as it was especially noticeable at high magnification (8000×). Moreover, DeV-IE presented more stripes, visible at 2000× magnification. Furthermore, the tubule density was slightly higher in DeV-D with respect to DeL-D (6200 tubules/$mm^2$, 4800 tubules/$mm^2$, respectively), while the orientation was similar in both areas (Fig. 5B). Finally, comparing Pe with De, PeV-D displayed the highest number of tubules, followed by PeL-D, DeV-D, and DeL-D.

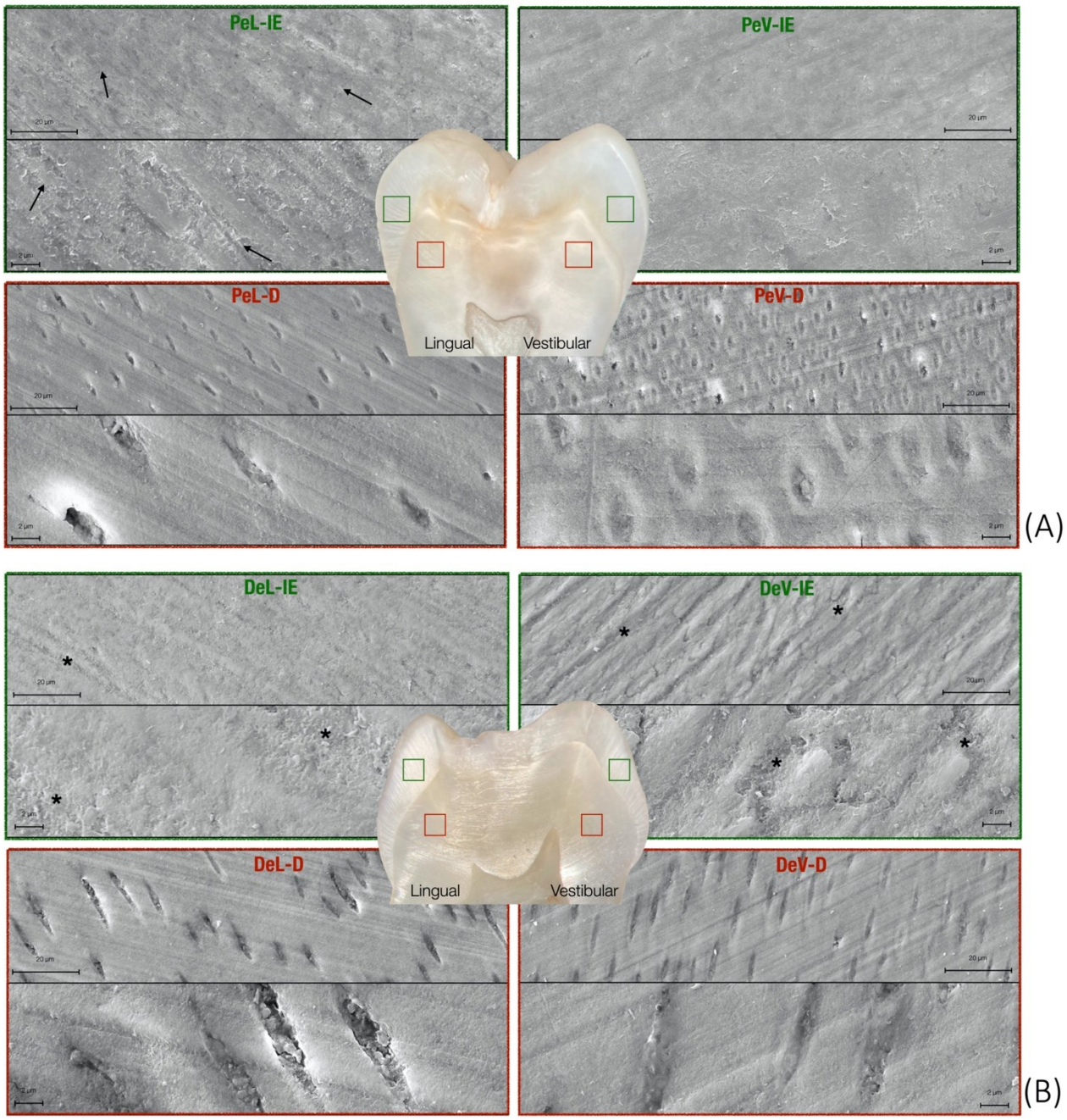


**Fig. 5**. Scanning electron micrographs of inner enamel and dentin of (A) Pe and (B) De collected at 2000× (upper micrographs of each colored case) and 8000× (lower micrographs of each colored case) original magnifications. (A) PeL-IE presented a more irregular surface with a partial loss of the enamel-like structure (black arrows), respect to PeV-IE, which displayed the most regular surface; PeL-D showed a lower number of dentinal tubules with respect to PeV-D. (B) DeL-IE displayed a partial loss of perikymata (black asterisks), more pronounced in DeV-IE, which presented at 2000× magnification more stripes. The dentinal tubule density was slightly higher in DeV-D with respect to DeL-D.

The EDS investigation of Ca, P, O, C, Mg and Na were reported in Fig. 6 as mean (wt%) ± SD. As regards Ca and P, lower values were observed in dentin regions, with respect to enamel ones

($p<0.05$). No statistically significant changes ($p>0.05$) were observed in the amount of O in all the analyzed areas, except for DeV-OE which displayed the highest one ($p<0.05$). Higher values of C and Mg were found in dentin of both Pe and De with respect to enamel ($p<0.05$); moreover, C displayed a higher amount in PeL-D and PeV-D than DeL-D and DeV-D ($p<0.05$); PeV-OE showed a major content of C respect to PeL-OE, PeL-IE, PeV-IE ($p<0.05$); DeV-OE and DeL-OE displayed higher C values respect to DeV-IE and DeL-IE ($p<0.05$). As regards Na, the highest values were presented by PeL-IE, PeL-D, PeV-D, DeL-D, DeV-IE, and DeV-D ($p<0.05$), while the lowest was shown in DeV-OE ($p<0.05$).

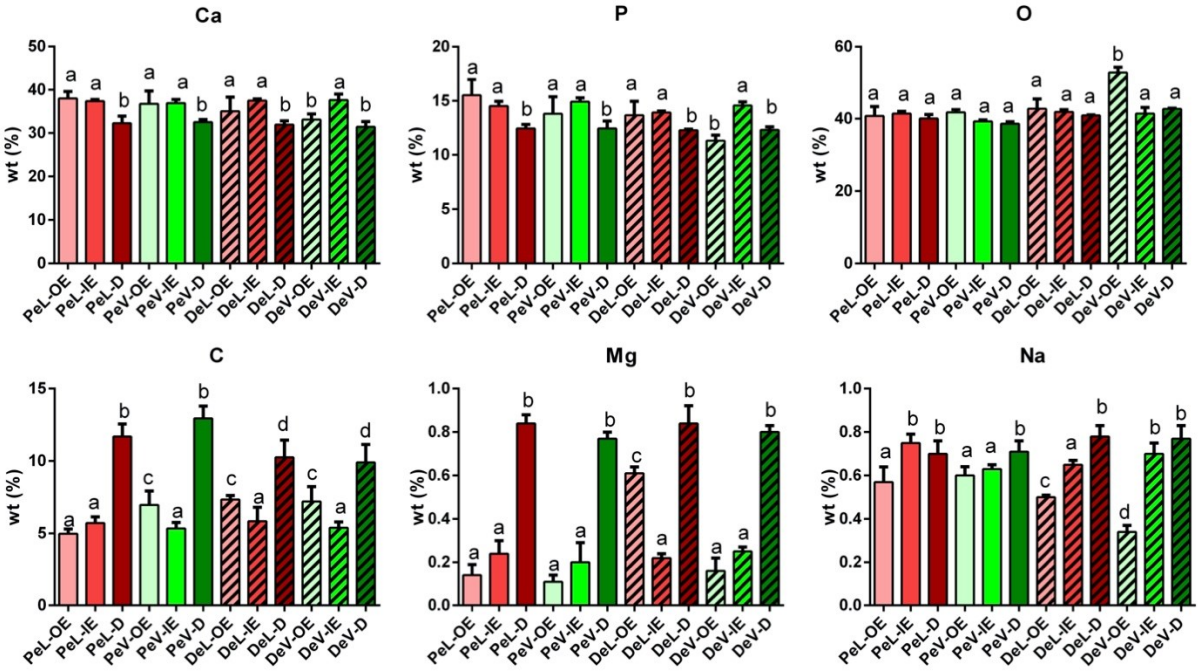


**Fig. 6**. EDS analysis of internal regions of lingual and vestibular sides of Pe and De. Mean element analysis by EDS spot measurements: calcium (Ca); phosphorous (P); oxygen (O); carbon (C); magnesium (Mg), and sodium (Na). Data are presented as mean (wt%) ± SD; different uppercase letters indicate statistically significant differences among groups ($p < 0.05$; Chi square test).

PCR was performed to correlate the modifications in the Raman spectral profiles of Pe and De (reported respectively in Fig. 7A and 7B) to EDS results. First, PCA was employed as an unsupervised multivariate approach to analyze Raman spectra of all teeth internal regions. Fig. 7C and 7D display the obtained PC scores plot and the PC1 and PC2 loadings, respectively. Complete segregation of spectra from dentin and enamel regions was obtained along PC1 (62.8% of explained variance); PC2 (15.6% of explained variance) completely discriminates enamel of Pe and De. No separation was found according to vestibular and lingual surfaces. The loading spectra of PC1 and PC2 axes report how the most discriminant spectral features are ascribable to the following Raman peaks: 1660 $cm^{-1}$ (Amide I peak of proteins), 1070 $cm^{-1}$ ($CO_3^{2-}$ groups), 1005 $cm^{-1}$ (phenylalanine of the organic

matrix), and 960 $cm^{-1}$ ($PO_4^{3-}$ groups of HA) [6]. Then, PC scores were used to create a regression model able to correlate the spectral information with EDS values (wt% of calcium, phosphorous, oxygen, carbon, magnesium, and sodium). Very good linear correlations were found for phosphorous ($R^2$=0.944) and oxygen ($R^2$=0.810); satisfactory linear correlations were observed also for calcium ($R^2$=0.543) and magnesium ($R^2$=0.522); finally, $R^2$ values lower than 0.35 were displayed by carbon ($R^2$=0.335) and sodium ($R^2$=0.260).

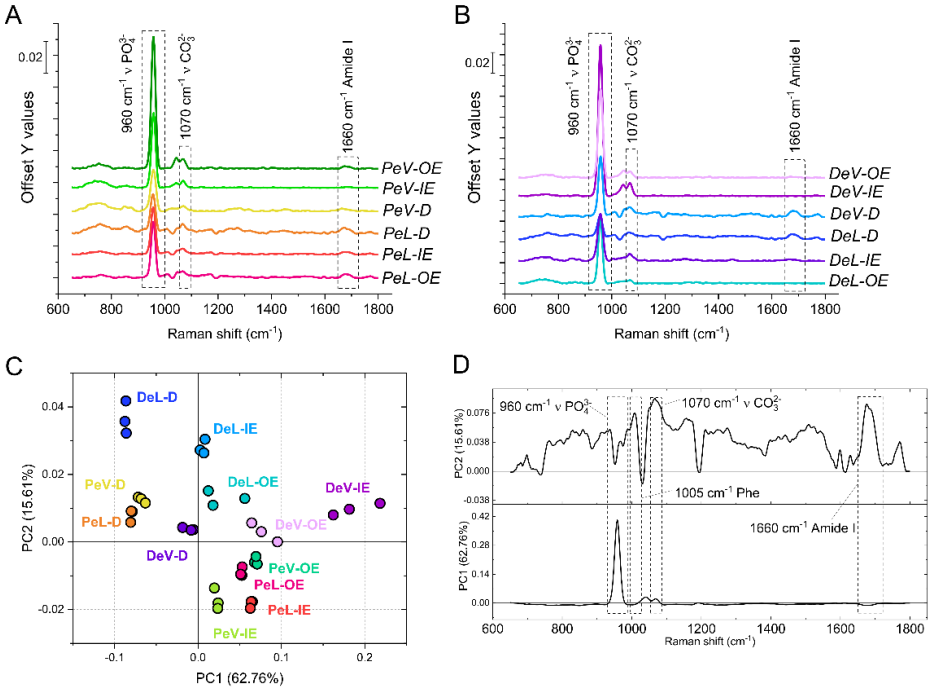


**Fig. 7.** Analysis of internal regions of lingual and vestibular surfaces of Pe and De. Average Raman spectra of (A) Pe and (B) De. In A and B dotted rectangles highlight the three peaks of interest; for better viewing, spectra are offset along the y-axis. (C) PCA scores plot and (D) corresponding PC1 and PC2 loading spectra.

## 4. Discussion

In the present study, for the first time, to the best of authors' knowledge, a multidisciplinary approach, combining Raman MicroSpectroscopy, Scanning Electron Microscopy, Energy Dispersive X-ray Spectrometry, and Vickers microHardness test, was exploited to define the chemical/elemental composition and microstructure of vestibular and lingual sides in Pe and De [4,13].

The analysis was first focused on the external enamel surface. It has been reported by the scientific literature that permanent enamel is richly formed by enamel prisms [13], while deciduous one is characterized by a lower prismatic density, with also smaller prisms, lower mineral substances, and major organic content [30,31]. However, these previous studies did not distinguish between lingual

and vestibular sides. In the present research, Pe were characterized by some irregularities in the enamel microstructure, more pronounced in the lingual side with respect to the vestibular one, associated with lower VMH values, probably ascribable to the mechanical and acid deterioration occurring during human life, which promotes dental demineralization [32,33].

As regards De, both surfaces showed a microstructure with a partial loss of typical perikymata. Interestingly, differences in RMS profiles were displayed between Pe and De; in particular, PeL and PeV exhibited different RMS spectral populations, while no difference was highlighted between DeL and DeV, probably due to their lower lifetime, which is not sufficient to alter their chemical composition.

To better investigate these differences, the analysis of the internal regions, of both lingual and vestibular sides, was exploited. The chemical composition was evaluated by the following specific RMS parameters: Mineral/Matrix, Crystallinity, and C/P, whose distribution was highlighted by means of false-color images.

The Mineral/Matrix ratio was higher in Pe than in De, with the highest values showed by inner and outer enamel of permanent vestibular side and the lowest by dentin of deciduous one. According to EDS spot measurements, the amount of P, representative of the mineral component, was similar in the outer and inner enamel of lingual and vestibular sides of Pe and De, except for DeV-OE, which presented a lower value. The different mean concentration of P in Pe and De is reported in literature [6,7,34]. According to Cuy et al., P decreases from outer to inner enamel, while Na and Mg increase towards the dentin-enamel junction [23]. Noteworthy, these authors considered the inner enamel as the region close to the dentin-enamel junction, while, for the present study, the inner enamel was referred to as the central area between outer enamel and dentin-enamel junction. Thus, these differences may be due to several factors, such as the area of the tooth in which data were collected.

Moreover, the irregular enamel area, displayed in particular in De, respect to Pe, probably promotes the ions and molecules diffusion, playing a crucial role in the dynamics of the caries process and susceptibility, as well as during teeth restorations [35]. It is indeed well-known that due to the lower mineralization of deciduous enamel compared to the permanent one, processes of erosion and decay happen mostly and more rapidly in De respect to Pe [36].

Crystallinity is correlated to the degree of order within the crystals and represents a critical component of HA, since ions' substitution may introduce structure distortions. According to our findings, the lowest values of crystallinity were displayed by dentin regions, while homogenous values were found in the inner and the outer enamel regions of both vestibular and lingual sides, in Pe and De. By comparing crystallinity with the C/P ratio, the increase in carbonate content was associated with a decrease in crystallinity, in agreement with Xu et al [37]. In fact, carbonate is a significant substituent in the crystal structure of biological HA [23,38], occupying the position either of the hydroxyl ($OH^-$) groups (type A carbonated HA) or of the phosphate ($PO_4^{3-}$) groups (type B carbonated HA) [39]. A previous study reported that, although carbonate ions can cause a distortion

of the apatite crystal lattice in both positions, it is less tightly bound in type A, contributing to greater solubility of enamel [39]. In our study, the C/P ratio was higher in outer enamel with respect to inner one and in the lingual side respect to the vestibular one, both in Pe and De; as regards dentin, the C/P ratio was lower in Pe than De and no differences were found between the lingual and the vestibular sides. These findings could be explained by considering the position of the carbonate in the HA crystal [29]. Since outer enamel of Pe and De showed higher values of C/P than the corresponding inner ones, the substitution of carbonate in HA crystal could probably be the effect of the acidic environment of the oral cavity. Since the outer enamel of Pe contains high amounts of B-type carbonate, the outer tooth surface is less soluble and more resistant to the attack from acids produced by dental plaque microorganisms that lead to dental decay [40]. Conversely, De contain a low rate of B-type carbonate, and hence they are more susceptible to the caries process [39]. In this light, as it is noticeable in RMS maps, the lower crystallinity and higher carbonate substitution in deciduous dentin might contribute to their lower hardness and might be partly compensated by higher collagen cross-linking of the matrix content [6]. The present results are also associated with a lower tubule density and higher intertubular dentin in De respect to Pe. Therefore, these findings could have relevant clinical implications, since the different chemical/elemental composition and morphological surfaces of De and Pe can influence the dental acidic demineralization process [41], the timing of the etching phase and the adhesive procedures [42]. Indeed, a mild self-etching adhesive system with a low acidic power [43,44], without a pre-etching phase, might be sufficient to promote adhesion to enamel and dentin of De. Furthermore, this simplified adhesive system could be the right choice also because it can be applied in a single clinical step, thus requiring less chair-time, which is certainly relevant in managing the behavior of pediatric patients [45]. On the contrary, a traditional etching phase could cause a deeper decalcification of the intertubular De dentin since its low mineral content, provoking a thicker hybrid layer and lower adhesive bond strength [45].

The statistical correlation found in the present study, between RMS spectral features and both VMH measurements and EDS data, offers an innovative tool for the analysis of human teeth. In fact, unlike SEM [46] and VMH [23] techniques, RMS represents a non-destructive procedure that allows collecting on the same sample, without fixing procedures, reliable and objective chemical and structural information, simplifying data acquisition and reducing times of analysis [47]. Recently, the use of RMS for biomedical applications, including dentistry, has significantly increased given the advantages in instrumentation and the development of fiber optic probes [23,29,37,47–49]. In this light, RMS could be proposed as an innovative method to diagnose early dental caries and other developmental defects affecting enamel and dentin [29], and to identify the degree of mineralization of teeth in order to choose the best adhesive and resin-based composite materials to be used for dental restorations. Although clinicians usually treat in the same way Pe and De, the remarkable chemical and structural differences highlighted in this study could lead to changes in preventive and restorative protocols. In fact, a deeper knowledge of teeth composition is mandatory to develop new bonding

strategies, mainly today, when minimally invasive adhesive dentistry is the final goal of dental practitioners [50]. The reduced number of analysed samples could be considered as a limitation of this study. However, further studies will be conducted to increase the knowledge on the structural and molecular features of Pe and De, regarding both the lingual and vestibular sides. The correlations found in this research add new and extremely useful information to the scientific literature related to operative dentistry, which could represent a relevant advance in the knowledge of the analytical approaches necessary to study the microstructure and the chemical/elemental composition of different calcified tissues, leading to other potential applications in clinics.

## 5. Conclusions

To date, very limited work has been done to compare the features of calcified tissues in human teeth, and no report has been focused on the differences between the vestibular and the lingual sides. This is the first study that describes, by means of a multidisciplinary approach based on different analytical techniques, the microstructure of enamel and dentin in Pe and De, evaluating both the vestibular and lingual sides. The information obtained on microhardness and chemical/elemental structure among the analyzed tooth samples, sheds new light on novel approaches in choosing dental materials with the best performance in clinical practice. Moreover, the consistency and reliability of the results obtained by RMS, with respect to all the other exploited analytical techniques, lead the way to the application of this vibrational technique as a diagnostic tool to identify anomalies or other diseases in calcified dental tissues.

**Author Contributions:** Giu O, RM, GO and AP conceptualization; Giu O, VN, RM, VT data curation; VN, VT, FV and GG formal analysis; GO and AP funding acquisition; investigation; Giu O, RM, VN, VT, FV, GG methodology; GO and AP project administration; VN, GG, AP resources; VN, GG software; GO and AP supervision; Giu O, RM, VN validation; Giu O, RM, VN, GO writing-review and editing.

**Funding:** SISOPD (Società Italiana Stomatologia, Odontoiatria e Protesi Dentaria-Italian Society of Dentistry, Stomatology and Prosthodontics) Foundation partially supported this study. The sponsor had no role on design, analysis, and interpretation of the study.

**Acknowledgments:** The authors extend their gratitude to Adriano Di Cristoforo (Department of Materials, Environmental Science, and Urban Planning, Polytechnic University of Marche, Ancona, Italy) for his precious support in SEM and EDS measurements.

**Conflicts of Interest:** The authors declare that they have no known competing financial interest or personal relationships that could have appeared to influence the work reported in this study. Authors

confirm that the submitted work, including images, is original and the journal policies have been reviewed. There are no conflicts of interest to disclose.

**Data Availability Statement:** The data presented in this study are available on request from the corresponding author G.O.

**References**


[1] A.L. Boskey, Biomineralization: an overview, Connect Tissue Res. 44 Suppl 1 (2003) 5–9.

[2] R.S. Lacruz, S. Habelitz, J.T. Wright, M.L. Paine, Dental Enamel Formation and Implications for Oral Health and Disease, Physiological Reviews. 97 (2017) 939–993. https://doi.org/10.1152/physrev.00030.2016.

[3] Ten Cate's Oral Histology - 9th Edition, (n.d.). https://www.elsevier.com/books/ten-cates-oral-histology/nanci/978-0-323-48524-1 (accessed February 20, 2021).

[4] M.A.H. De Menezes Oliveira, C.P. Torres, J.M. Gomes-Silva, M.A. Chinelatti, F.C.H. De Menezes, R.G. Palma-Dibb, M.C. Borsatto, Microstructure and mineral composition of dental enamel of permanent and deciduous teeth, Microsc Res Tech. 73 (2010) 572–577. https://doi.org/10.1002/jemt.20796.

[5] J. de D. Teruel, A. Alcolea, A. Hernández, A.J.O. Ruiz, Comparison of chemical composition of enamel and dentine in human, bovine, porcine and ovine teeth, Arch Oral Biol. 60 (2015) 768–775. https://doi.org/10.1016/j.archoralbio.2015.01.014.

[6] M. Anwar Alebrahim, C. Krafft, W. Sekhaneh, B. Sigusch, J. Popp, ATR-FTIR and Raman spectroscopy of primary and permanent teeth, Biomedical Spectroscopy and Imaging. 3 (2014) 15–27. https://doi.org/10.3233/bsi-130059.

[7] W.H. Arnold, P. Gaengler, Quantitative analysis of the calcium and phosphorus content of developing and permanent human teeth, Ann Anat. 189 (2007) 183–190. https://doi.org/10.1016/j.aanat.2006.09.008.

[8] A.F.S. Borges, R.A. Bitar, K.R. Kantovitz, A.B. Correr, A.A. Martin, R.M. Puppin-Rontani, New perspectives about molecular arrangement of primary and permanent dentin, Applied Surface Science. 254 (2007) 1498–1505. https://doi.org/10.1016/j.apsusc.2007.07.018.

[9] L.J. Wang, R. Tang, T. Bonstein, P. Bush, G.H. Nancollas, Enamel demineralization in primary and permanent teeth, J Dent Res. 85 (2006) 359–363. https://doi.org/10.1177/154405910608500415.

[10] M.L. Hunter, N.X. West, J.A. Hughes, R.G. Newcombe, M. Addy, Erosion of deciduous and permanent dental hard tissue in the oral environment, J Dent. 28 (2000) 257–263. https://doi.org/10.1016/s0300-5712(99)00079-2.

[11] A. Desoutter, A. Slimani, R. Al-Obaidi, S. Barthélemi, F. Cuisinier, H. Tassery, H. Salehi, Cross striation in human permanent and deciduous enamel measured with confocal Raman microscopy, Journal of Raman Spectroscopy. 50 (2019) 548–556. https://doi.org/10.1002/jrs.5555.

[12] K.V. Mortimer, The relationship of deciduous enamel structure to dental disease, Caries Res. 4 (1970) 206–223. https://doi.org/10.1159/000259643.

[13] E. Gentile, D. Di Stasio, R. Santoro, M. Contaldo, C. Salerno, R. Serpico, A. Lucchese, In vivo microstructural analysis of enamel in permanent and deciduous teeth, Ultrastruct Pathol. 39 (2015) 131–134. https://doi.org/10.3109/01913123.2014.960544.

[14] M. Marquezan, B.L. da Silveira, L.H. Burnett, C.R.M.D. Rodrigues, P.F. Kramer, Microtensile bond

strength of contemporary adhesives to primary enamel and dentin, J Clin Pediatr Dent. 32 (2008) 127–132. https://doi.org/10.17796/jcpd.32.2.l512r1p807w54582.
[15] A. Carden, M.D. Morris, Application of vibrational spectroscopy to the study of mineralized tissues (review), JBO. 5 (2000) 259–268. https://doi.org/10.1117/1.429994.
[16] C.P. Torres, J. Miranda Gomes-Silva, M.A.H. Menezes-Oliveira, L.E. Silva Soares, R.G. Palma-Dibb, M.C. Borsatto, FT-Raman spectroscopy, μ-EDXRF spectrometry, and microhardness analysis of the dentin of primary and permanent teeth, Microsc Res Tech. 81 (2018) 509–514. https://doi.org/10.1002/jemt.23005.
[17] J. Wang, W. Chen, Y. Jiang, J. Liang, Imaging of extraradicular biofilm using combined scanning electron microscopy and stereomicroscopy, Microsc Res Tech. 76 (2013) 979–983. https://doi.org/10.1002/jemt.22257.
[18] I. Świetlicka, M. Arczewska, S. Muszyński, E. Tomaszewska, M. Świetlicki, D. Kuc, M. Mielnik-Błaszczak, K. Gołacki, K. Cieślak, Surface analysis of etched enamel modified during the prenatal period, Spectrochimica Acta Part A: Molecular and Biomolecular Spectroscopy. 222 (2019) 117271. https://doi.org/10.1016/j.saa.2019.117271.
[19] T. Paradella, M. Bottino, Scanning Electron Microscopy in modern dentistry research, Brazilian Dental Science. 15 (2012). https://doi.org/10.14295/bds.2012.v15i2.798.
[20] G. Orilisi, V. Tosco, R. Monterubbianesi, V. Notarstefano, M. Özcan, A. Putignano, G. Orsini, ATR-FTIR, EDS and SEM evaluations of enamel structure after treatment with hydrogen peroxide bleaching agents loaded with nano-hydroxyapatite particles, PeerJ. 9 (2021) e10606. https://doi.org/10.7717/peerj.10606.
[21] A. Guentsch, M.D. Fahmy, C. Wehrle, S. Nietzsche, J. Popp, D.C. Watts, S. Kranz, C. Krafft, B.W. Sigusch, Effect of biomimetic mineralization on enamel and dentin: A Raman and EDX analysis, Dental Materials. 35 (2019) 1300–1307. https://doi.org/10.1016/j.dental.2019.05.025.
[22] I.S. Furlan, E.C. Bridi, F.L.B. do Amaral, F.M.G. França, C.P. Turssi, R.T. Basting, Effect of high- or low-concentration bleaching agents containing calcium and/or fluoride on enamel microhardness, Gen Dent. 65 (2017) 66–70.
[23] J.L. Cuy, A.B. Mann, K.J. Livi, M.F. Teaford, T.P. Weihs, Nanoindentation mapping of the mechanical properties of human molar tooth enamel, Arch Oral Biol. 47 (2002) 281–291. https://doi.org/10.1016/s0003-9969(02)00006-7.
[24] WMA - The World Medical Association-WMA Declaration of Helsinki – Ethical Principles for Medical Research Involving Human Subjects, (n.d.). https://www.wma.net/policies-post/wma-declaration-of-helsinki-ethical-principles-for-medical-research-involving-human-subjects/ (accessed January 31, 2021).
[25] M. Beyer, J. Reichert, B.W. Sigusch, D.C. Watts, K.D. Jandt, Morphology and structure of polymer layers protecting dental enamel against erosion, Dent Mater. 28 (2012) 1089–1097. https://doi.org/10.1016/j.dental.2012.07.003.
[26] A. Biancolillo, F. Marini, Chemometric Methods for Spectroscopy-Based Pharmaceutical Analysis, Front Chem. 6 (2018) 576. https://doi.org/10.3389/fchem.2018.00576.
[27] V. Notarstefano, G. Gioacchini, H.J. Byrne, C. Zacà, E. Sereni, L. Vaccari, A. Borini, O. Carnevali, E. Giorgini, Vibrational characterization of granulosa cells from patients affected by unilateral ovarian endometriosis: New insights from infrared and Raman microspectroscopy, Spectrochim Acta A Mol Biomol Spectrosc. 212 (2019) 206–214. https://doi.org/10.1016/j.saa.2018.12.054.
[28] V. Notarstefano, S. Sabbatini, C. Conti, M. Pisani, P. Astolfi, C. Pro, C. Rubini, L. Vaccari, E. Giorgini,

Investigation of human pancreatic cancer tissues by Fourier Transform Infrared Hyperspectral Imaging, J Biophotonics. 13 (2020) e201960071. https://doi.org/10.1002/jbio.201960071.
[29] R. Ramakrishnaiah, G. ur Rehman, S. Basavarajappa, A.A.A. Khuraif, B.H. Durgesh, A.S. Khan, I. ur Rehman, Applications of Raman Spectroscopy in Dentistry: Analysis of Tooth Structure, Applied Spectroscopy Reviews. 50 (2015) 332–350. https://doi.org/10.1080/05704928.2014.986734.
[30] A. Lucchese, G.P. Pilolli, M. Petruzzi, V. Crincoli, M. Scivetti, G. Favia, Analysis of collagen distribution in human crown dentin by confocal laser scanning microscopy, Ultrastruct Pathol. 32 (2008) 107–111. https://doi.org/10.1080/01913120801897216.
[31] M. Contaldo, D. Di Stasio, R. Santoro, L. Laino, L. Perillo, M. Petruzzi, D. Lauritano, R. Serpico, A. Lucchese, Non-invasive in vivo visualization of enamel defects by reflectance confocal microscopy (RCM), Odontology. 103 (2015) 177–184. https://doi.org/10.1007/s10266-014-0155-4.
[32] A.S. Pereira, L.R.S. Lima, M. de D.M. de Lima, C.C.B. Lima, S.M. Paiva, L. de F.A. de D. Moura, M.S. de Moura, Consumption of Acidic Beverages is a Predisposing Factor for Erosive Tooth Wear in Preschool Children: A Population-based Study, Oral Health Prev Dent. 18 (2020) 1061–1067. https://doi.org/10.3290/j.ohpd.b871069.
[33] I.-A. Meira, E.-J.-L. Dos Santos, N.-L.-S. Fernandes, E.-T. de Sousa, A.-F.-B. de Oliveira, F.-C. Sampaio, Erosive effect of industrialized fruit juices exposure in enamel and dentine substrates: An in vitro study, J Clin Exp Dent. 13 (2021) e48–e55. https://doi.org/10.4317/jced.57385.
[34] M.A.H. De Menezes Oliveira, C.P. Torres, J.M. Gomes-Silva, M.A. Chinelatti, F.C.H. De Menezes, R.G. Palma-Dibb, M.C. Borsatto, Microstructure and mineral composition of dental enamel of permanent and deciduous teeth, Microsc Res Tech. 73 (2010) 572–577. https://doi.org/10.1002/jemt.20796.
[35] A.G.R. Targino, A. Rosenblatt, A.F. Oliveira, A.M.B. Chaves, V.E. Santos, The relationship of enamel defects and caries: a cohort study, Oral Dis. 17 (2011) 420–426. https://doi.org/10.1111/j.1601-0825.2010.01770.x.
[36] A.K. Johansson, R. Sorvari, D. Birkhed, J.H. Meurman, Dental erosion in deciduous teeth--an in vivo and in vitro study, J Dent. 29 (2001) 333–340. https://doi.org/10.1016/s0300-5712(01)00029-x.
[37] C. Xu, R. Reed, J.P. Gorski, Y. Wang, M.P. Walker, The Distribution of Carbonate in Enamel and its Correlation with Structure and Mechanical Properties, J Mater Sci. 47 (2012) 8035–8043. https://doi.org/10.1007/s10853-012-6693-7.
[38] E.A. Abou Neel, A. Aljabo, A. Strange, S. Ibrahim, M. Coathup, A.M. Young, L. Bozec, V. Mudera, Demineralization–remineralization dynamics in teeth and bone, Int J Nanomedicine. 11 (2016) 4743–4763. https://doi.org/10.2147/IJN.S107624.
[39] Developmental and Histological Aspects of Deciduous and Young Permanent Teeth - Management of Dental Emergencies in Children and Adolescents - Wiley Online Library, (n.d.). https://onlinelibrary.wiley.com/doi/abs/10.1002/9781119372684.ch1.1 (accessed February 3, 2021).
[40] H.-B. Pan, B.W. Darvell, Calcium Phosphate Solubility: The Need for Re-Evaluation, Crystal Growth & Design. 9 (2009) 639–645. https://doi.org/10.1021/cg801118v.
[41] M. Kuhar, P. Cevc, M. Schara, N. Funduk, Enhanced permeability of acid-etched or ground dental enamel, J Prosthet Dent. 77 (1997) 578–582. https://doi.org/10.1016/s0022-3913(97)70098-2.
[42] W. Tesch, N. Eidelman, P. Roschger, F. Goldenberg, K. Klaushofer, P. Fratzl, Graded microstructure and mechanical properties of human crown dentin, Calcif Tissue Int. 69 (2001) 147–157.

https://doi.org/10.1007/s00223-001-2012-z.
[43] N. Akimoto, M. Takamizu, Y. Momoi, 10-year clinical evaluation of a self-etching adhesive system, Oper Dent. 32 (2007) 3–10. https://doi.org/10.2341/06-46.
[44] A.F.S. Borges, R.M. Puppin-Rontani, R.A. Bittar, K.R. Kantowitz, F.M. Pascon, A.A. Martin, Effects of acidic primer/adhesives on primary and permanent dentin, Am J Dent. 22 (2009) 30–36.
[45] M. Ebrahimi, A. Janani, S. Majidinia, R. Sadeghi, A.S. Shirazi, Are self-etch adhesives reliable for primary tooth dentin? A systematic review and meta-analysis, J Conserv Dent. 21 (2018) 243–250. https://doi.org/10.4103/JCD.JCD_287_17.
[46] E.R. Fischer, B.T. Hansen, V. Nair, F.H. Hoyt, D.W. Dorward, Scanning Electron Microscopy, Curr Protoc Microbiol. CHAPTER (2012) Unit2B.2. https://doi.org/10.1002/9780471729259.mc02b02s25.
[47] C. Krafft, V. Sergo, Biomedical applications of Raman and infrared spectroscopy to diagnose tissues, (2012). https://doi.org/10.1155/2006/738186.
[48] A.C.-T. Ko, L.-P. Choo-Smith, M. Hewko, M.G. Sowa, C.C.S. Dong, B. Cleghorn, Detection of early dental caries using polarized Raman spectroscopy, Opt Express. 14 (2006) 203–215. https://doi.org/10.1364/opex.14.000203.
[49] Y.H. El-Sharkawyi, Detection and Characterization of Human Teeth Caries Using 2D Correlation Raman Spectroscopy, J Biomed Phys Eng. 9 (2019) 167–178. https://www.ncbi.nlm.nih.gov/pmc/articles/PMC6538916/ (accessed February 11, 2021).
[50] G. Orsini, V. Tosco, R. Monterubbianesi, G. Orilisi, A. Putignano, A New Era in Restorative Dentistry, in: S. Longhi, A. Monteriù, A. Freddi, L. Aquilanti, M.G. Ceravolo, O. Carnevali, M. Giordano, G. Moroncini (Eds.), The First Outstanding 50 Years of "Università Politecnica Delle Marche": Research Achievements in Life Sciences, Springer International Publishing, Cham, 2020: pp. 319–334. https://doi.org/10.1007/978-3-030-33832-9_21.